Elemental ratios as tracers of the sources of mineral dust in north-eastern Sahara

M. Boraiy, M. El-Metwally, A. Borbon, S. Chevaillier, B. Laurent, S. Lafon, F. El Sanabary, M. Masmoudi, S. Alfaro

HAL Id: hal-04256544

https://hal.u-pec.fr/hal-04256544v1

Submitted on 9 Nov 2023

ORIGINAL PAPER

Elemental ratios as tracers of the sources of mineral dust in north-eastern Sahara

M. Boraiy[1] · M. El-Metwally[2] · A. Borbon[3] · S. Chevaillier[4] · B. Laurent[5] · S. Lafon[5] · F. F. El Sanabary[1] · M. Masmoudi[6] · S. C. Alfaro[4]

Abstract

The objective of this study is to confirm the possibility of tracing sources of airborne mineral dust using elemental ratios. The region of study is the north-eastern part of the Sahara where dust compositional data were lacking; 272 mineral dust samples collected at 3 experimental stations of Egypt were analyzed by X-ray fluorescence. Based on the mineral dust concentration, 65% of the samples correspond to moderate ($3–10\ \mu g\ m^{-3}$), 22% to medium ($10–25\ \mu g\ m^{-3}$), and 13% to intense ($> 25\ \mu g\ m^{-3}$) dust events. The Ca/Al and (Mg + Ca)/Fe ratios were found to be strongly correlated and their ranges of variation to cover are more than one order of magnitude, which confirms their interest for the tracing of the dust sources. Using a combination of MODIS satellite observations, HYSPLIT back-trajectory analysis, and simulations with dust emission models, the large (> 6) and intermediate ($2–6$) Ca/Al ratios were shown to correspond to dust originating from saline playas (chotts) and calcareous surfaces, respectively. Conversely, the lowest (< 2) ratios correspond to dust emitted by siliceous sand seas (ergs). Therefore, a classification of the dust in 3 categories (erg-like, calcareous, and chott-like) based on Ca/Al is proposed. The events of moderate to medium intensity are dominated by chott-like and calcareous dust, which suggests that these sources are activated during erosion events of limited (local) extension. Conversely, the fact that the dust composition is more likely to be of the erg-like type during intense events underlines the dominant role played by sand dune fields during major erosion events.

1 Physics and Mathematical Engineering Department, Faculty of Engineering, Port Said University, Port Said, Egypt

2 Physics Department, Faculty of Science, Port Said University, Port Said, Egypt

3 Laboratoire de Météorologie Physique, UMR6016, Université Clermont Auvergne, OPGC, CNRS, 63000 Clermont-Ferrand, France

4 Univ Paris Est Creteil and Université Paris Cité, CNRS, LISA, 94010 Créteil, France

5 Université Paris Cité and Univ Paris Est Creteil, CNRS, LISA, 75013 Paris, France

6 Faculty of Sciences of Sfax, Sfax University, Soukra Road, 3038 Sfax, Tunisia

Introduction

According to the most recent estimates yielded by 16 models of the Coupled Model Intercomparison Project (CMIP6), the emission of mineral dust (MD) by wind erosion in the arid or semiarid areas of the World contributes annually from 1374 to 7571 Tg to the atmospheric particulate loading (Zhao et al. 2022). The size of these particles ranges from about 0.1 to more than 20 μm (Kandler et al. 2009), and their residence time does not exceed 1 week to 10 days in the troposphere (Knippertz and Stuut 2014; Schepanski 2018). Because of this limited duration and also of the sporadic emissions, the MD concentrations are highly heterogeneous in space and time. They are the largest in the source areas, and immediately downwind of them, and thus represent a health hazard for the populations (Griffin et al. 2001; Morman and Plumlee 2013). Nonetheless, a significant part of the mineral particles can be transported hundreds or thousands of kilometers from their source region (Al-Harbi 2015;

Issanova et al. 2015; Knippertz et al. 2015; Suresh et al. 2022). Because the wind-erodible fraction of the topsoil is enriched in nutrients, this departure decreases the productivity of the parent soil (Li et al. 2007). Conversely, in the areas where dust deposition occurs, the terrestrial or marine ecosystems may benefit from the input of fresh nutrients necessary for their development (Okin et al. 2004; Schulz et al. 2012). This is, for instance, the case of the Amazonian forest (Swap et al. 1992) and of the marine regions in which the biological productivity is limited by the scarcity of elements such as P or Fe (Okin et al. 2004; Jickells et al. 2005; Cassar et al. 2007; Rodríguez et al. 2011). Among the latter, the Eastern Mediterranean Sea is one of the most oligotrophic of the world ocean (Varkitzi et al. 2020) and its biological productivity is largely dependent on the atmospheric inputs of nutrients (Richon et al. 2018).

During their transport from the source to the deposition zones, dust particles impact the Earth's climate directly by scattering and/or absorbing the solar and terrestrial radiation (Sokolik et al. 2001; Balkanski et al. 2007) and indirectly by acting as cloud condensation or ice nuclei and thus modifying the radiative properties of clouds (Kumar et al. 2011). MD is also suspected of playing a major role in atmospheric chemistry through modifications of the actinic flux (Bian and Zender 2003) and by being involved in heterogeneous reactions with highly reactive gaseous species (Dentener et al. 1996).

In summary, MD is an essential component of the Earth system whose emission/transport/deposition cycle must be perfectly understood, described, and modeled if one wants to quantify its complex effects on the environment. The large range of yearly emission predicted by the CMIP6 models shows that the uncertainties on the modeling of the dust cycle are still important. Another point that the current models overlooked until quite recently was the elemental or mineralogical composition of the emitted dust, which is problematic because composition conditions in great part the optical properties of the dust and also the inputs of nutrients to the ocean. In an attempt to address this issue, Menut et al. (2020) considered for instance that the composition of the dust was identical to that of the source soil and coupled the map of soil mineralogy proposed by Journet et al. (2014) with the version of the CHIMERE chemistry-transport model described in Mailler et al. (2017). However, the assumption underlying this method disregards the compositional fractionation occurring during emission. An alternative solution to the question of the composition would consist in attributing to the dust of each one of the major source areas of the World a composition based on in situ observations. This approach was employed by Scheuvens et al. (2013) who compiled the data of the literature related to the main dust sources identified in North Africa. They showed that the compositions of both the source sediments

and dust samples were highly variable and that some clear regional trends could be observed. Unfortunately, for lack of soil or dust samples collected in most of the Sahara and along all the Mediterranean coast, no data were available to characterize directly the dust composition in the northernmost part of the African continent, which is to say at the beginning of its transport path toward the Mediterranean Sea and Europe (Moulin et al. 1998; Bibi et al. 2020). Later on, this gap was filled in part for the Central Mediterranean region by Saad et al. (2018) who characterized the elemental composition of 190 dust samples collected in Central Tunisia on the island of Kerkennah and at the experimental site of Sfax University and confirmed the results of Scheuvens et al., namely that a selection such elemental ratios as Ca/Al and (Mg + Ca)/Fe appeared as relevant tracers of the dust source regions.

Over at least the last 180.000 years, there were 2 major routes of dust export toward the Eastern Mediterranean: a first one transporting Arabian dust along a south-east/north west axis and a second one carrying Saharan dust from its Sahelian, Libyan, and Egyptian sources toward the northeast (Ammar et al. 2014; Ben-Israel et al. 2015). During the relatively wet historical periods of the past, the Arabian route prevailed, but in the drier ones—as is now the case—the Saharan route dominates (Ehrmann and Schmiedl 2021). Unfortunately, the composition of the mineral dust transiting along this currently prevailing pathway has never been documented directly. The rare pieces of information available concern dust deposited in Cairo (Linke et al. 2006), in Israel (e.g., Ganor and Foner 1996) and in Jordan (Abed et al. 2009).

The overall aim of this study is to perform for the northeastern part of the Sahara an analysis of the dust composition similar to that made by Saad et al. (2018) in Tunisia. More precisely, X-ray fluorescence (XRF) analysis was used to document the bulk elemental composition of the dust collected at the Egyptian experimental stations of Port Said University (229 samples), Cairo University (32 samples), and El Farafra (11 samples). To supplement this dataset, two dust samples (SR and WD, respectively) were also generated in the laboratory from soils collected along the Mers Matruh to Siwa road (at lat.: 29.95°N, lon.: 25.99°E) and in the White Desert (lat.:27.20°N, lon.: 28.06°E), north of the El Farafra Oasis. In a second stage, we propose to establish a link between the elemental composition of the dust and the type of source soil from which it was produced.

Information on the locations of the experimental sites, and on the dust sampling and generation protocols is provided in "Materials and methods" section. It also details the elemental analysis by XRF. Then, an in-depth analysis of the variabilities of both the dust concentration and composition is developed in "Results and discussion" section. In discussion, the results obtained in Egypt are compared with those

of other Saharan regions, and a typology of dust sources based on the Ca/Al ratio is proposed. Finally, the conclusion section summarizes the main results of this study and suggests new ideas of research to supplement it.

Materials and methods

General context and location of the sampling sites

The majority of the Egyptian population live along the fertile valley of the Nile River and in its delta. The Western and Eastern Deserts, separated by the Nile (Fig. 1), and the Sinai Peninsula occupy the rest of the country. From a simplified geological point of view, the soils of the Western Desert and of the northern part of the Eastern Desert are predominantly carbonates whose formation dates back to the Eocene and the Miocene (Hamimi et al. 2020). In the classification of the Food and Agricultural Organization (FAO), they are mostly distributed into 3 categories: gleyik yermosols, solonchaks, and sand dunes (Yk, Zo, and DS, respectively, in Fig. 1). With the notable exception of the Qattara Depression (> 50 000 km^2 appearing in pink color in Fig. 1) and of smaller

depressions (Siwa, Fayum, Bahariya, Farafra, Dakhla, and Kharga) whose bottom is covered by a mixture of salts and sand, the plateaus of the Western Desert are relatively flat. On its western side, the wind-fed Great Sand Sea covers more than 70.000 km^2 and extends well into Libya, and the composition of its sand grains overwhelmingly dominated by quartz is similar to that of all the other Saharan ergs (Pastore et al. 2021). This combination of factors (flat topography, large supply of wind-erodible material) explains that the Western Desert coincides with one of the major sources of dust in the eastern part of the Sahara (Caquineau et al. 2002). Conversely, the Egyptian desert east of the River Nile (Eastern Desert) and the Sinai Peninsula are characterized by a more complex mountainous topography that is less favorable to wind erosion. Along the coasts of the Suez Gulf and the Red Sea, the composition of the lithosols (l in Fig. 1) is principally dominated by igneous and metamorphic rocks.

The regular winds blowing most of the year over Egypt are from the north-west to north-east sector (El-Wakil et al. 2001; El-Askary and Kafatos 2008; El-Metwally et al. 2008; El-Metwally and Alfaro 2013). However, in their analysis of the 562 cyclones born over the Sahara between 1980 and 2009, Ammar et al. (2014) showed that the tracks of the
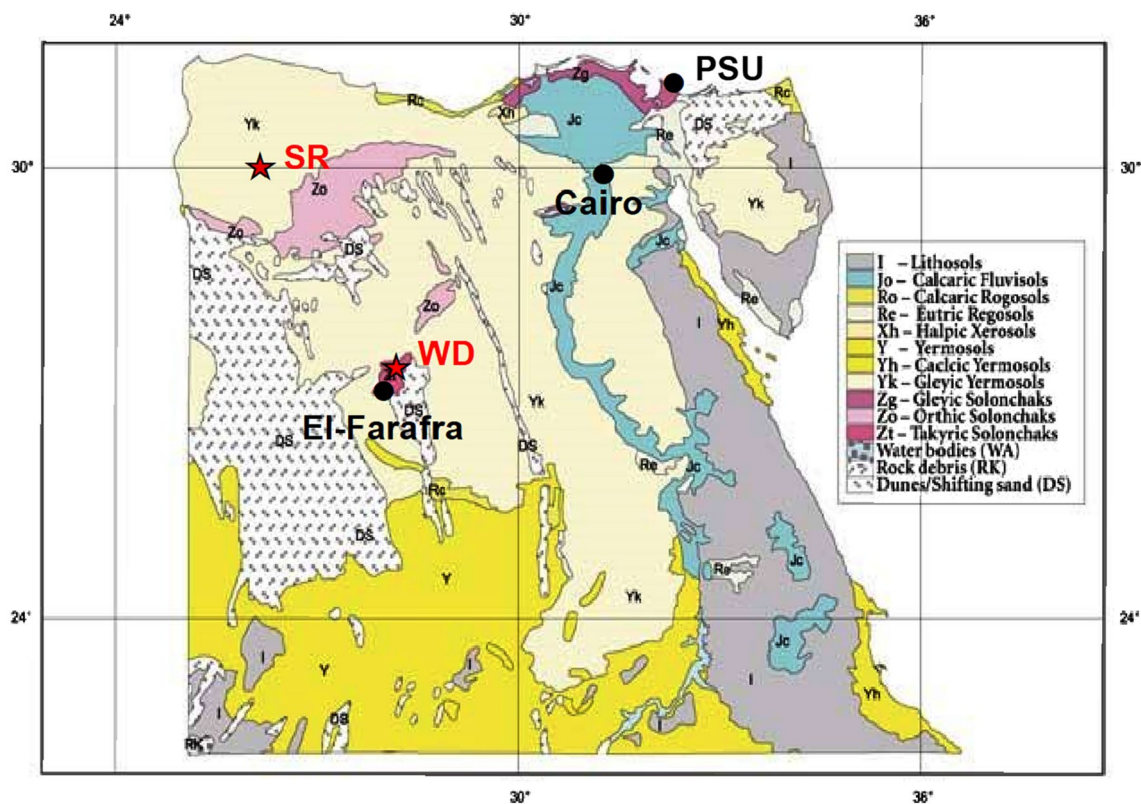

Fig. 1 Food and Agricultural Organization (FAO) classification of the Egyptian soils (Source: DSMW-FAO-UNESCO, https://www.fao.org/3/y5863e/y5863e05.htm). The locations of the Port Said University (PSU), Cairo University (Cairo), and El Farafra Meteorological station (El Farafra) where the aerosol samples were collected are reported. The two stars indicate the places (SR for Siwa road, and WD for White Desert) where the soil samples used for the dust generation in the laboratory were taken

55% having at least a portion of their trajectory above the Egyptian territory were preferentially oriented either along a west/north-east direction (toward the Eastern Mediterranean and the Middle East), or along a west/east axis (in direction of Arabia). The strong surface winds associated with these depressions are called Khamaseen winds by the Egyptians. They are more frequent in spring (March, April, and May) and raise huge clouds of desert dust whose optical characteristics derived from sunphotometer observations performed at the experimental sites of the Port-Said University (PSU), Cairo University in Giza (Cairo), and Egyptian Meteorological Authority station of El Farafra are well documented in the literature (El-Metwally and Alfaro 2013; El-Metwally et al. 2008; El-Metwally et al. 2010, 2011, 2020), respectively.

These 3 sites were also equipped for collecting samples of the airborne material on filters suitable for the subsequent determination of the elemental composition of the desert dust by X-ray fluorescence analysis. Port Said is located on the Mediterranean coast at the northern end of the Suez Canal. The conurbation of Port Said and Port Fouad hosts about 1 million inhabitants and many industrial activities. It is under the wind of the Western Desert sources of dust when winds blow from the west to south-west sectors (El-Metwally and Alfaro 2013). With its population of more than 25 million and concentrating most of Egypt's industrial activities, the Greater Cairo area is one of the most polluted megacities in the world (e.g., Wheida et al. 2018; Mostafa et al. 2019). In addition, inputs of mineral dust from the Western Desert contribute, depending on the season, from 35 to 65% of the particulate matter atmospheric loading (Favez et al. 2008). Conversely, El Farafra has the smallest population (ca. 10.000) of all Egyptian oases. It is located far from any major source of anthropic pollution but is directly under the wind of the Great Sand Sea or the Qattara Depression when winds come from the south-west to north-west or north sectors, respectively. The White Desert (see Fig. 1 in the supplementary material), which is a former sea bed very rich in chalk and gypsum (hence its name) and prone to deflation, is about 40 km north of El Farafra. Under north winds, it can also be a source of mineral particles for the El Farafra sampling site.

Sampling protocol and quantification of the elemental composition

At Cairo University (Giza, Egypt), 53 aerosol samples were collected on the terraced roof of the Physics department (Lat.: 30.02°N, Lon.: 31.20°E, Elev.: 19 m a.m.s.l.) during the spring 2005 intensive observation periods of the Cairo Aerosol CHaracterization Experiment (CACHE) (Alfaro and Abdel Wahab 2005). The sampling inlet had a cutoff size of 10 μm, and the particles were collected on poly-carbonate membranes with pore size of 0.4 μm (Nuclepore, Whatman™) at a flow rate of 1 m^3/h. The sampling duration was about 3 h during the day and 15 s every minute for twelve hours (thus also amounting to 3 h in all) during the night. The actual volume sampled necessary for the calculation of the concentrations was measured with a gas meter (model 2000, Gallus).

The same procedure was used at PSU (Lat.: 31.27°N; Lon.: 32.28°E; Elev.; 21 m amsl), the only difference being that the pumping was always sequential (on for 5 min every hour) and each sampling period lasted 24 h. At El Farafra (Lat.: 27.06°N; Lon.: 27.99°E, Elev.: 92 m amsl), the pumping was turned on and off manually, and the sampling duration varied from 2 to 24 h. In all, 350 daily samples were collected at PSU between February 2015 and September 2018 and 11 at El Farafra (5 in April 2015 and 6 in July 2016).

Then, wavelength-dispersive X-ray fluorescence (WD-XRF) performed with a Panalytical spectrometer (model PW-2404) was used to analyze the elemental compositions of the aerosols collected on the membranes. In the instrument, the primary X-rays are produced by a Coolidge tube ($I_{max} = 125$ mA, $V_{max} = 60$ kV) with a Rh anode. The membranes are introduced into the spectrometer without any special preparation. The method is non-destructive, fast (3 repetitions of 10 s), and multi-elemental. The results of the analyses were corrected for two types of blank membrane counts (blanks of the laboratory where the filters were changed, and field blanks). The quantification limit (QL) of each element is determined as being 10 times the standard deviation of the measurements performed on the blank membranes. Fifteen elements were quantified: Na, Mg, Al, Si, P, S, Cl, K, Ca, Ti, Fe, Ni, Cu, Zn, and Pb.

In this study, Al is of particular interest because it is known to be an ideal tracer of mineral dust (Alfaro et al. 2003a; Scheuvens et al. 2013; Marconi et al. 2014) and can be used to quantify the overall mineral dust concentration (MD) (Taylor 1964):

$$MD = Al/0.08 \qquad (1)$$

For the crustal elements having also a possible marine origin (e.g., Ca, Mg, and K), estimating the part of their concentration associated with mineral dust requires subtracting the share due to sea salt. This is particularly important in coastal environments such as Port Said and can be done using their elemental ratio in sea salt relative to Na$_{ss}$, which is the concentration of Na corresponding to sea salt.

Na$_{ss}$ is obtained using the average value (0.1) of the (Na/Al) ratio in desert aerosols (Bowen 1966):

$$Na_{ss} = Na - 0.1\ Al \qquad (2)$$

Then,

$$Ca_{dust} = Ca - \left(\frac{Ca}{Na}\right)_{ss} Na_{ss} \tag{3}$$

$$Mg_{dust} = Mg - \left(\frac{Mg}{Na}\right)_{ss} Na_{ss} \tag{4}$$

$$K_{dust} = K - \left(\frac{K}{Na}\right)_{ss} Na_{ss} \tag{5}$$

For the ratios $(Ca/Na)_{ss}$, $(Mg/Na)_{ss}$, and $(K/Na)_{ss}$ the values (0.038, 0.129, and 0.037, respectively) recommended by Henderson and Henderson (2009) and used in Marconi et al. (2014) were retained.

In the following, all the Ca, Mg, and K concentrations will be systematically corrected but that, for simplicity, the subscript 'dust' will be omitted. Note that there would still be an overestimation of the concentrations of the elements for which an anthropogenic contribution is possible, particularly in urban areas. For instance, biomass burning is known to release K, and to a lesser extent Mg (e.g., Maenhaut et al. 1996; Alfaro et al. 2003b).

Generation of aerosols in the laboratory

The chemical composition of the dust sampled on site can be compared with that of the dust generated from soil samples with the GAMEL generator (Lafon et al. 2014). Only 1 g of soil is necessary for the experiments. It is introduced inside a 500-mL filtering flask moved by a mechanical wrist-action shaker (Agitest ®, 8 mm-amplitude) and the ensuing collisions liberate the fine fraction of the soil aggregates. After passing through a cyclone of the URG type and of 10 µm nominal aerodynamic diameter cut-off, the aerosol-sized particles are collected on the same polycarbonate filters (pore size 0.4 µm) as those used on field. One of the advantages of the laboratory generation is that there can be no doubt as to the origin of the particles, whereas the identification of the origin of the dust collected outdoor is a much more complex task (cf., next sub-section). The method was already used by Saad et al. (2018) who had compared the elemental composition of the dust collected along the Tunisian coast with that of particles produced in the laboratory from soils sampled in Algeria, Libya, and in Douz (Tunisia). The latter soil is of particular interest for the present study because of its vicinity with the Chott El Jerid, a vast sebkha whose saline nature compares to that of the Qattara Depression.

Origin of the dust sampled onsite

Particularly during the most important dust storms, the dust-laden air-masses may have received particles from several sources located along their path before being sampled at the experimental stations. Therefore, it is often impossible to link the collected dust to a unique and precise source area. However, 3 different methods can be combined to provide some hindsight on the geographical origin of the dust: (1) the examination of the images of satellite-borne instruments such as MODIS aboard Aqua and Terra can be used to confirm the presence of a dust plume over the experimental site. These images can be easily accessed via the NASA Earth data portal (https://worldview.earthdata.nasa.gov/), (2) the mapping of the dust plumes provided by reanalyses can be used to locate the areas of largest surface concentrations. In this work, we use both Version 2 of the Modern-Era Retrospective Analysis for Research and Applications (MERRA-2) of the Global Modelling and Assimilation Office (GMAO 2018), and the regional BSC DREAM8b, which is one of the most commonly used models to forecast dust event in North Africa, Mediterranean, and Middle-East regions (Basart et al. 2012), and (3) the trajectories of the dust-laden air masses reconstructed using the HYSPLIT model (Stein et al. 2015) in the backward mode. Hysplit is accessible directly online via the NOAA website (https://www.ready.noaa.gov/HYSPLIT.php). Dust simulations with MERRA-2 and BSC-DREAM8b are done for different purposes (long term dust study vs. operational forecasting, respectively) and are based on different parameterizations to model dust. Nevertheless, it is interesting to point out that combining simulation outputs like it is done by operational modeling centers allows to illustrate the consistency of dust products. Here, it will be shown that the models agree to simulate the source areas of major dust outbreaks.

Results and discussion

Dust concentration at the 3 sampling sites

The application of Eq. (1) to the 350 Al concentrations measured at PSU yields MD values ranging from 0.85 to 266.5 µg m^{-3}. The focus of this study being on mineral dust, the very low MD concentrations were not considered. As in Saad et al. (2018), the inferior limit was set at 3 µg m^{-3}, which left 229 daily samples for the dust characterization. Among the samples collected in Cairo, 32 passed the same selection criterion and the MD ranged between 3.1 and 130.9 µg m^{-3}. Finally, with their MD between 6.9 and 250.4 µg m^{-3}, all the 11 samples of the El Farafra station were retained.

Table 1 Characteristics of the frequency distributions of the mineral dust concentrations (MD, in µg m^{-3}) measured at the 3 Egyptian experimental sites

Stations	N	Min	Max	10th percentile	50th percentile	90th percentile	%Moderate	%Medium	%Intense
Port Said	229	3.0	266.5	3.5	6.8	24.5	69	21	10
Cairo	32	3.1	130.9	4.6	12.1	73.7	41	31	28
El Farafra	11	6.1	250.4	6.9	13.1	84.8	45	18	36
Sfax	132	3.0	103.9	3.8	7.5	24.5	66	24	10

For comparison, the values obtained by Saad et al. (2018) at the Tunisian coastal city of Sfax are also reported

Table 1 reports the indicators (Min., Max., 10th, 50th, and 90th percentiles) of the statistical distribution of the MD values available at the 3 sites. As expected, the MD mean seems to be larger in the middle of the Western Desert (El Farafra) than at the downwind locations of Cairo and Port Said, but this would need to be confirmed with more than 11 samples. More interestingly, the peaks of MD are of the same order of magnitude (> 100 µg m^{-3}) at all sites, which confirms that the influence of the strongest dust events is felt much beyond the area of the dust sources. Also noteworthy, the 10th, 50th, and 90th percentiles of the MD distribution for Port Said (3.5, 6.8, and 24.5 µg m^{-3}, respectively) are quite similar to those obtained (3.8, 7.5, and 24.5 µg m^{-3}, respectively) from the data collected by Saad et al. (2018) at the Tunisian coastal city of Sfax (Table 1). As in the latter study, 'intense' events will be defined as having MD exceeding 25 µg m^{-3}. They represent 10% of the dust cases at Port Said and Sfax, 28% at Cairo, and 36% at El Farafra. In the following, two categories will be distinguished among the less intense cases: the 'moderate' ($3 < MD < 10$ µg m^{-3}) and the 'medium' ($10 < MD < 25$ µg m^{-3}) ones.

Elemental composition

The correlation between the concentrations of the most important crustal elements (Si, Ca, Fe, Ti, Mg, K, and P) and that of Al was quantified by the means of Pearson's coefficient of determination (r^2). With its $r^2 > 0.99$ (Table 2), Si is found to be quasi-perfectly proportional to Al at the three experimental sites. In the case of Fe, r^2 is also very close to 1 (> 0.96) except at PSU where the correlation is somewhat weaker ($r^2 = 0.91$). In order to understand why, the evolution of Fe/Al with MD at PSU is compared (Fig. 2) to those at the 3 sites where the correlation of Fe with Al is the strongest. There is no significant difference between Cairo, El Farafra, and Sfax, but at PSU a clear enrichment in Fe is observed at low MDs. This suggests the presence in the city of a background concentration of iron of probable anthropogenic origin that needs to be subtracted from the overall Fe concentrations to obtain the share really associated with mineral dust. This correction is particularly important for the computation of the

($Mg + Ca$)/Fe ratio that is very sensitive to errors on the Fe concentration. In the following, the Fe/Al values larger than the average + 1 standard deviation ($0.78 + 0.19$) of the measurements at the other 3 sites will be considered as suspicious and be replaced by the average (0.78) in the calculation of the dust elemental ratios involving Fe. Practically, this replacement is necessary only at low MDs for which the relative weight of the non-dust iron is the largest.

In the best of our knowledge, there is no work in the literature documenting directly the X/Al (in which the symbol X stands for any crustal element other than Al) ratios of airborne dust sampled in Egypt. The only available data with which to compare the values of Table 2 are those of Linke et al. (2006) and Abed et al. (2009). In their study, the former authors quantified the elemental compositions of the fine (PM20) fractions of (1) one sample of soil collected 75 km north-east of Cairo and (2) one sample of dust deposited in Cairo after an intense dust event. Following the original publication, these two samples will be referred to (Table 3) as Cairo 2 and Cairo 3, respectively. Abed et al. (2009) analyzed the composition of dust deposits collected in 10 localities of Jordan after at least 5 major Khamaseen storms having reached the country in spring 2006. Thus, the analyzed dust was assumedly of Saharan origin.

In addition, the composition of the dust sampled onsite can be compared to that of aerosols generated with GAMEL (Table 3) from the Egyptian soils collected at two different locations of the Western Desert (Siwa Road and White Desert; this work) and from the Tunisian soil (Douz; data from Saad et al. 2018).

From one site to the other and independently of the nature (airborne, soil, or deposit) of the dust sample, the ranges of variation in Fe/Al and Ti/Al are limited (Tables 2, 3). This relative constancy confirms Scheuvens et al's (2013) conclusion that these elemental ratios are not appropriate to trace the origin of mineral dust. The P/Al ratio is between 0.01 and 0.101 in all the samples except in the dust generated from the White Desert soil for which it is unusually large (0.74). Although this would need to be more thoroughly investigated, this could be explained by the presence in this former sea bed of biological P (fish bones and scales) similar

Table 2 Mean and standard deviation (SD) of the ratios to Al of 7 crustal elements measured in the airborne dust sampled at the 3 Egyptian stations of this study and at the Tunisian coastal city of Sfax (data from Saad et al. 2018)

| Ref	Country	Site		Si/Al	Fe/Al	Ti/Al	Ca/Al	Mg/Al	K/Al	P/Al
This work	Egypt	Port Said	Mean (SD) r^2	3.32 (0.58) 0.99	1.10 (0.36) 0.91	0.12 (0.05) 0.92	4.47 (2.33) 0.44	0.58 (0.20) 0.86	0.57 (0.44) 0.65	0.05 (0.02) 0.22
This work	Egypt	Cairo	Mean (SD) r^2	4.01 (0.48) 0.99	0.81 (0.33) 0.96	0.21 (0.06) 0.97	3.07 (1.10) 0.95	0.26 (0.07) 0.96	0.32 (0.10) 0.97	0.04 (0.07) 0.32
This work	Egypt	El Farafra	Mean (SD) r^2	2.68 (0.24) 0.99	0.66 (0.16) 0.99	0.07 (0.01) 0.99	4.08 (2.72) 0.38	0.29 (0.03) 0.99	0.27 (0.06) 0.99	0.03 (0.02) 0.81
Saad et al. (2018)	Tunisia	Sfax*	Mean (SD) r^2	3.22 (0.38) 0.99	0.79 (0.15) 0.97	0.08 (0.01) 0.98	5.72 (2.14) 0.28	0.45 (0.23) 0.87	0.43 (0.23) 0.87	0.02 (0.03) 0.19
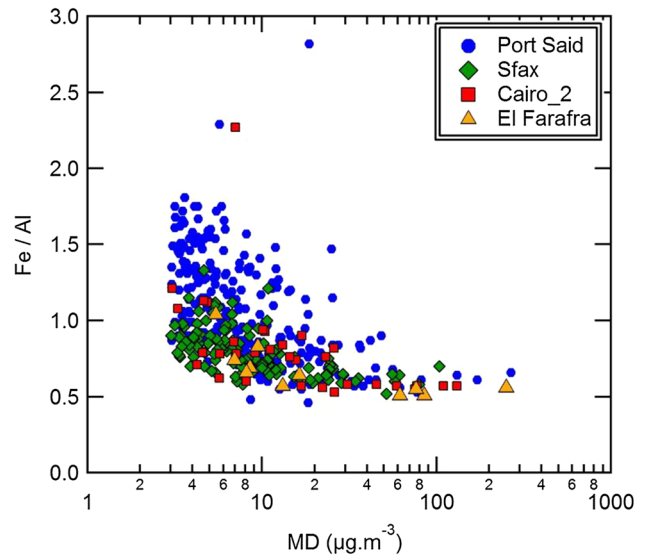
Fig. 2 Evolution of the Fe/Al ratio with the mineral dust concentration (MD) at the 3 Egyptian sampling sites of this study. For comparison, the data acquired at Sfax (Tunisia) by Saad et al (2018) are also reported

to that found in the Bodele Depression paleo-lake (Hudson-Edwards et al. 2014).

In Linke et al., Si/Al is significantly larger than in the samples of dust sampled on field or generated in GAMEL. Two reasons can explained this: (1) the diameters of the particles characterized by Linke et al. went up to 20 μm, whereas the cutoff size of the inlets was 10 μm at the 3 sampling stations and in GAMEL and (2) the coarsest dust particles are known to be enriched in quartz (SiO_2) (e.g., Kandler et al. 2009).

Conversely, the particularly poor correlation between Al and such elements as Ca, P, and to a lesser degree Mg denotes a more important variability of their X/Al ratios. Indeed, Ca/Al and P/Al are found to clearly decrease when MD increases at the 3 sites (Fig. 3a, b). This could indicate that during the moderate and medium dust events, mineral dust originates from sources richer in Ca and P than during the intense events. For Mg/Al (Fig. 3c), the decrease with MD is observed only at PSU but not at the Cairo or El Farafra sampling sites, which suggests (1) a limited sensitivity of this ratio to the nature of the dust source and (2) a probable anthropogenic contribution to the low Mg concentrations in Port Said. Finally, the large range of variation in (Mg + Ca)/Fe (Fig. 3d) emphasizes its potential interest as a tracer of the origin of the dust.

Despite its limited number of dust samples (11), the dataset collected at El Farafra seems particularly interesting for evidencing the influence of the source region on the dust composition. Indeed, the 11 representative points of this station in Fig. 3a, b, , d can be sorted into two groups: the first

Springer

Table 3 Elemental ratios of (1) the fine fraction (PM20) of one Egyptian soil (Cairo 2), (2) dust deposited in Cairo (Cairo 3) and in Jordan (10 sites), and (3) dust generated in the laboratory from 1 Tunisian (Douz) and 2 Egyptian soils of the Western Desert (Siwa Road and White Desert)

Ref	Country	Site	Si/Al	Fe/Al	Ti/Al	Ca/Al	Mg/Al	K/Al	P/Al
Linke et al. (2006)	Egypt	Cairo 2	6.32	0.77	0.21	4.26	0.43	0.24	0.021
		Cairo 3	5.82	0.70	0.14	2.00	0.57	0.28	0.018
Abed et al. (2009)	Jordan	10 sites	3.07–6.18	0.60–0.89	0.08–0.20	2.36–6.05	0.34–1.54	0.20–0.33	0.021–0.101
Saad et al. (2018)	Tunisia	Douz	2.87	0.82	–	6.16	0.29	–	0.012
This work	Egypt	Siwa Road	2.64	0.66	0.08	3.72	1.24	0.26	0.013
This work	Egypt	White Desert	1.57	0.77	–	53.6	0.78	0.59	0.74

Fig. 3 Evolution of the Ca/Al, P/Al, Mg/Al, and (Mg + Ca)/Fe ratios with the mineral dust concentration (MD) at the 3 Egyptian sampling sites: Port Said (PSU), Cairo (C2), and El Farafra(ElF) of this study
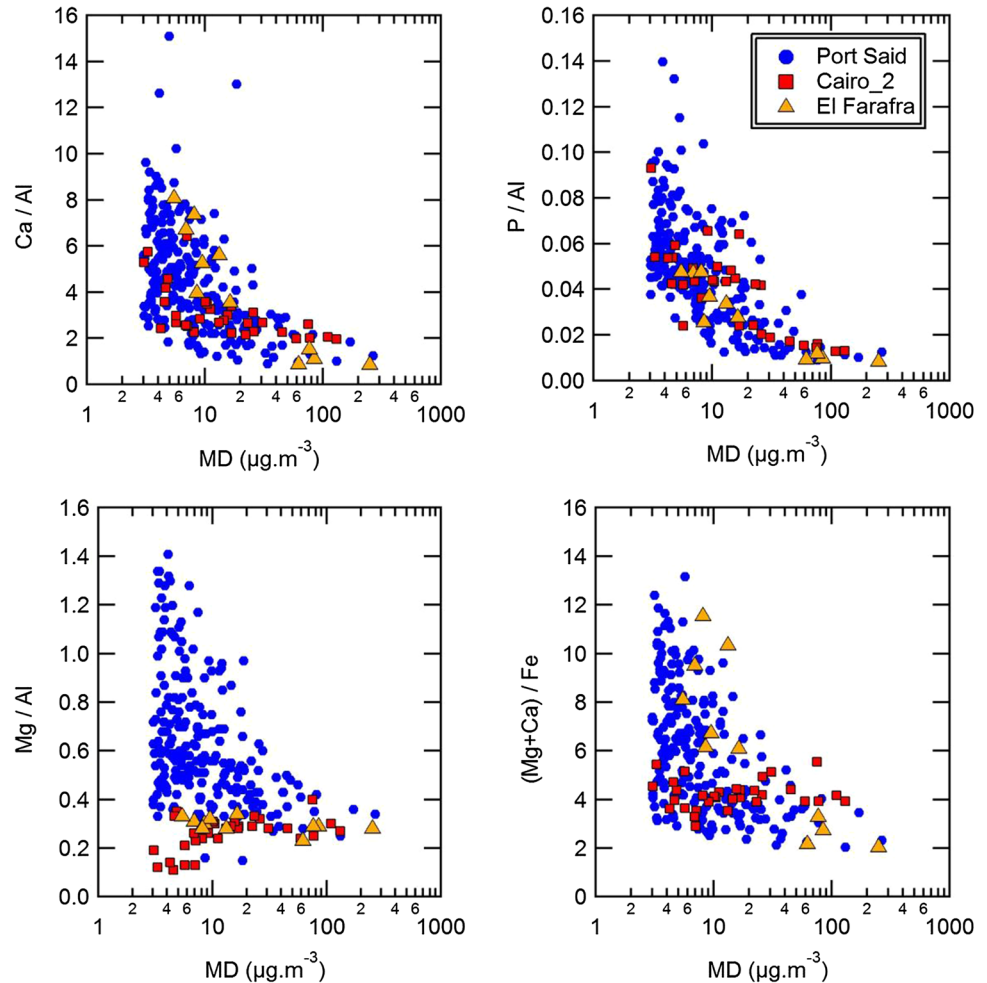
group (G1) containing 7 points (the 6 points acquired in July 2015 + that of 7 April 2016) of relatively low MDs and large Ca/Al, P/Al, and (Mg + Ca)/Fe ratios, whereas the second group (G2) of 4 points (all acquired in April 2016) corresponds to intense events of significantly lower X/Al ratios.

The reconstruction with the HYSPLIT model of the back-trajectories of the air-masses reaching the sampling site during the 7 periods of G1 shows that they were systematically coming from the north, which is to say from the direction of the Qattara Depression (the left column of Fig. 4 illustrates

the case of 5 July 2015). The MERRA-2 reconstruction of the dust concentration close to the surface also indicates the presence of dust plumes in the north of the Western Desert (Fig. 4b). Finally, the BSC-DREAM8bsimulations confirm that the dust emission condition was reached at least during the afternoon, when the surface winds are the strongest. Therefore, though moderate, emission was active in these periods and the emitted dust could be transported toward El Farafra. Conversely, during the 4 samplings of G2 the air-masses came from the west/south-west sector, which is to

say from the Great Sand Sea that was actively emitting dust in this period according to the MERRA-2 and BSC-DREAM8b simulations (The right-hand side of Fig. 4 illustrates the case of 9 April 2016). The dust plume produced by this intense event is also clearly visible on the MODIS images (Fig. 4b), which was not the case during the more moderate events of July 2015.

This analysis confirms the link between the elemental composition of the dust and its source region. More precisely, the Ca/Al, P/Al, and (Ca + Mg)/Fe ratios of the dust coming from the Great Sand Sea are notably smaller (1.09 ± 0.31, 0.010 ± 0.001, and 2.55 ± 0.58, respectively) than those of the dust coming from the Qattara Depression (5.80 ± 1.69, 0.038 ± 0.009, and 8.36 ± 2.16, respectively).

Discussion

The ranges of variation in the Ca/Al and (Mg + Ca)/Fe ratios measured at the three Egyptian sites of this study are consistent with the few data for this region summarized in the review of Scheuvens et al. (2013) and with the more extensive ones of Saad et al. (2018) for Tunisia. Importantly, these variations cover about one order of magnitude and the analysis of the El Farafra samples showed that their low and high extremes can be linked to the origin of the dust.

At least in the vast region extending from Tunisia to Egypt, these two potential source tracers are not independent. Indeed, (Mg + Ca)/Fe can be rewritten as:

$$((Mg + Ca)/Fe) = (Mg/Al + Ca/Al)/((Fe/Al)) \qquad (6)$$

As previously discussed, Fe/Al is fairly constant in our area of study and the results of Table 2 show that Mg/Al is about one order of magnitude lower than Ca/Al. Therefore, the variations in (Mg + Ca)/Fe are expected to be driven mostly by those of Ca/Al. This is confirmed by the quasi-linear inter-dependency of the two ratios visible, Fig. 5, on which all the data of Tables 2 and 3 are reported. Though characterized by its very large Ca/Al and (Mg + Ca)/Fe values, which can be linked to the overwhelming proportions of calcium carbonate and gypsum in this very specific area of the Western Desert, the point corresponding to the dust generated from the White Desert soil sample is aligned with the other points. The points representing the dust samples collected in Niger by Rajot et al. (2008) and Formenti et al. (2008) are also reported in Fig. 5. Despite their very low elemental ratios, these points representing Sahelian dust are also well aligned with the others. This linearity shows that Ca/Al or (Mg + Ca)/Fe could be used indifferently for tracing the origin of the dust. However, in the following Ca/Al will be preferred to (Mg + Ca)/Fe because its calculation does not involve any correction of a possible anthropogenic contribution to the Fe concentration.

The mineral dust coming to El Farafra from the Great Sand Sea, or to Sfax from the Algerian sand dunes (Area #3 in Saad et al.), is characterized by a very low Ca/Al (< 2). Conversely, the Ca/Al ratio of the dust arriving from the saline plains of Egypt (e.g., the Qattara Depression) or Tunisia (Chott El Jerid) is in the upper range of the observed values. These commonalities show that it is possible to propose a typology of the sources based on the Ca/Al ratio of the dust. Numerically, dust from sand dunes (erg-like dust) will correspond to Ca/Al < 2 and dust from saline areas (chott-like dust) to Ca/Al > 6.

The dust generated from the calcareous soils of the Siwa Road (this study) and the fine fraction of the soil collected north-east of Cairo by Linke et al. (2006) have Ca/Al values (3.72 and 4.26, respectively) located between these two extremes. Therefore, a first explanation for the intermediate (2 < Ca/Al < 6) values of Fig. 5 could be that they correspond to dust emitted by these 'calcareous' soils that cover most of the surface of the Western Desert outside the Great Sand Sea or the saline areas of which the Qattara Depression is the largest representative. However, another possibility would be that the corresponding dust is a mixture of particles produced from difference types of sources. In this case, the resulting Ca/Al would depend on the proportions of the mixture.

Using these numerical criteria, a type of dust source (erg-like, calcareous-like, or chott-like) can be proposed (Table 4) for the dust collected during the intense, medium, and moderate events recorded at PSU and Sfax.

As seen previously (Fig. 3a), Ca/Al tends to decrease with MD, which is to say with the intensity of the dust events. This is consistent with the absence of chott-like dust during the intense events recorded at PSU and Sfax (Table 4). Conversely, in the category of the moderate events that represents about two thirds (66 and 68%) of all cases at PSU and Sfax, the proportion of erg-like dust is very low (6 and 1%, respectively). These moderate events are neatly dominated by chott-like dust at Sfax (79%) but by calcareous dust (62%) at PSU where the proportion of chott-like dust is only 33%. This difference of influence of the saline areas on the composition of the dust collected at the two sampling sites is most probably due to their different distances to the source areas: Sfax is about 200 km directly under the wind of the Chott El Jerid, whereas Port Said is 400 km from the Qattara Depression.

A possible explanation for the lack of chott-like dust during the intense events is that these events are created by depressions whose influence is not purely local but at least regional. This means that the strong winds associated with these depressions activate simultaneously all the types of sources present within a relatively vast area. Among these
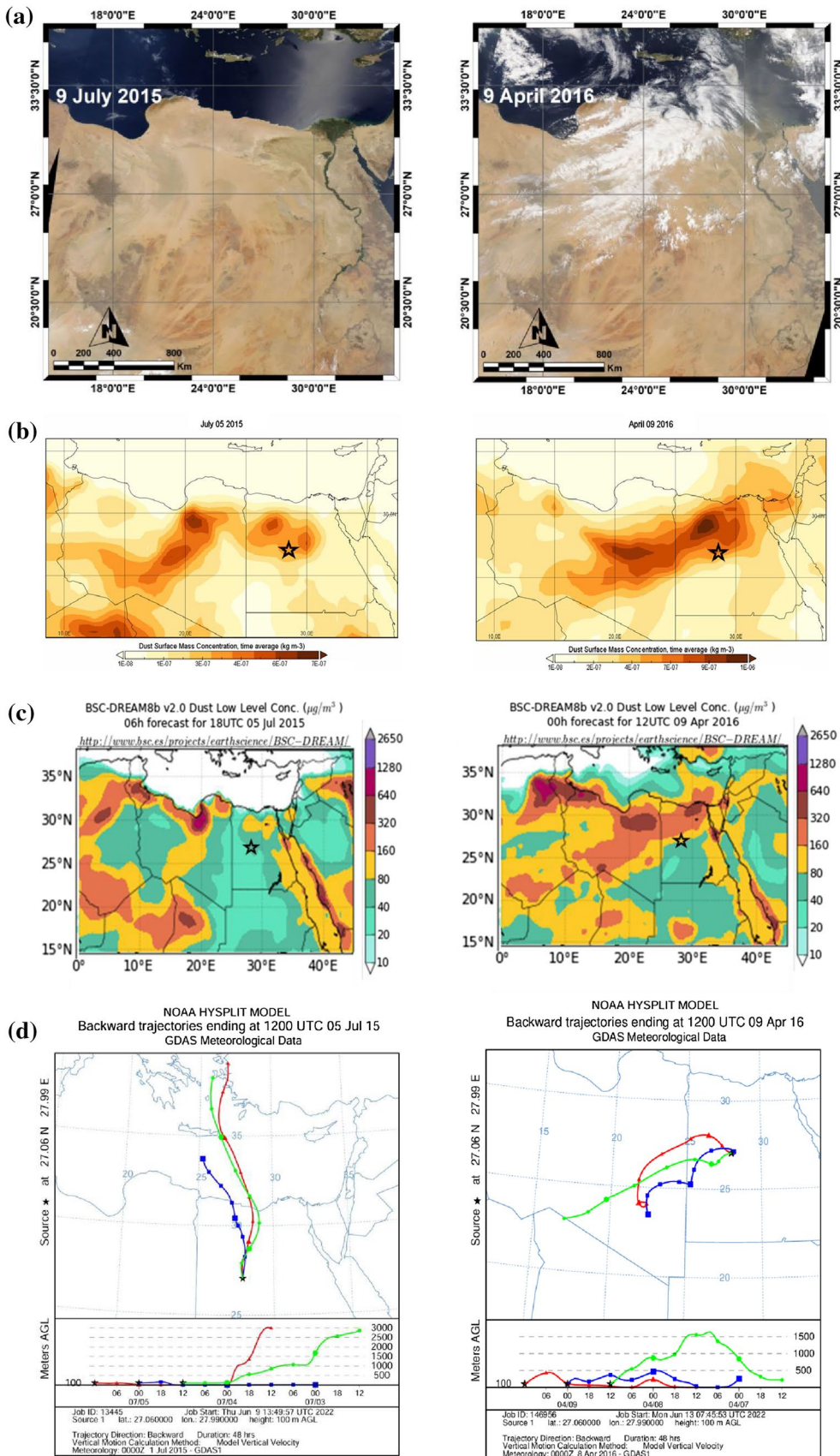
(a)

(b)

(c)

(d)

Fig. 4 Comparison of the conditions prevailing during one moderate (5 July 2015, left column) and one intense (9 April 2016, right column) events sampled at the station of El Farafra (star symbol). The first row (**a**) displays the Modis observations for these two days, the second and third ones (**b**, **c**), the MERRA-2 reanalysis surface concentrations (note the difference of scale in the two images) and the regional BSC-DREAM8b dust surface concentrations that both point out dust in the region of the Great Sand Sea overlapping the border between Libya and Egypt in the case of the intense event. Wind direction is visualized through the reconstruction of the air-masses trajectories with Hysplit (**d**)

sources, the sand dunes are the most readily mobilized because of their low threshold of erosion. Therefore, they emit more dust than the other surfaces and the mixture of dust raised by the strongest depressions is dominated by dust of the erg-like type. The smaller scale wind outbreaks have more chance of raising dust that comes only from the saline or calcareous areas. These outbreaks lead to moderate or medium concentrations, but they are more frequent than the intense events, which are relatively rare (Table 4).

Conclusion

Past studies had documented the composition of the mineral dust sampled in different parts of the Sahara and the Sahel and evidenced the regional variability of at least some of its elemental ratios, which suggested that these ratios could be used as tracers of the origin of the dust. In this work, we analyzed 272 dust samples collected in Egypt and compare their composition with that of 132 samples collected in Tunisia by Saad et al. (2018). In both cases, Ca/Al and (Mg+Ca)/Fe are strongly and linearly correlated and their ranges of variability cover more than one order of magnitude. This confirms the interest of using either one of them for the identification of the dust source, but we retained Ca/Al because it is insensitive to a possible anthropic contribution to the Fe concentration.

On average, Ca/Al is found to be larger and also more variable during the moderate and medium events (MD < 25 μg m^{-3}), than during the intense ones. Our interpretation of this observation is that the majority of the less intense events are caused by erosion occurring in areas of limited spatial extension. Therefore, the composition of the dust is able to reflect the variability of the composition of the soils in the area of study: the largest Ca/Al values are associated with saline playas (chott or sebkha), intermediate ones with carbonates, and the smallest ones with sand dunes (ergs).

Conversely, the intense events of the northern part of the Sahara are created by strong depressions moving toward the east. Because these particular meteorological conditions have a more extended outreach than local winds, they affect large desert areas with a variety of surface states (roughness,

size of the erodible grains, humidity, etc.) and composition. Therefore, the dust associated with these intense events should theoretically be a mixture of different dust types produced from the local sources. However, erosion is expected to be much more active over the erg-like surfaces because the threshold of erosion of the sand dunes is significantly lower than that of the other surface types (Laurent et al. 2008). This dominance most probably explains the commonalities of composition of the dust sampled during the intense events and the fact that this dust has the compositional characteristics of the erg-like dust (i.e., low Ca/Al ratios). Noteworthy, this interpretation is also consistent with the remarkable homogeneity of the physical properties (size distribution, complex refractive index, single scattering albedo, etc.) of the dust raised by the most intense events of the vast Sahara/Sahel/Arabian Peninsula area (Masmoudi et al. 2015).

In summary, our results show that it is possible to ascribe to different ranges of Ca/Al ratios not an unambiguously localized source area, but a type of dominant emitting surface: chott-like, calcareous, or erg-like. In future studies, it would be useful to document more completely the characteristics of the dust associated with these three types of sources: mineralogical composition, contents in nutrients, apportionment of the share of these nutrients soluble in sea water, etc. Based on the modeling of the dust emission, transport, and deposition, a quantification of the contribution of the 3 source types to the inputs of dust in the oligotrophic marine areas of the Mediterranean Sea would also be necessary
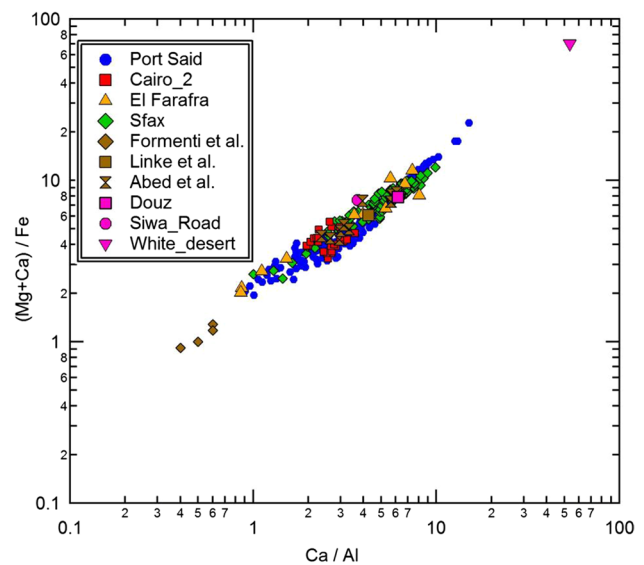

Fig. 5 Correlation between the (Mg+Ca)/Fe and Ca/Al ratios of the mineral dust sampled at 3 Egyptian (PSU, Cairo, and El Farafra) and one Tunisian (Sfax) sites. The values of the dust generated in the laboratory with GAMEL (Siwa Road, White Desert, and Douz) or reported in previous studies for the north-eastern Sahara (Linke et al. 2006; Abed et al. 2009) or the Sahel (Formenti et al. 2008) are also indicated

Table 4 Results of the apportionment of the Port Said and Sfax dust events according to their intensity (intense, medium, and moderate) and dust source type (erg, calcareous, and chott)

	PSU			Sfax		
	Intense	Medium	Moderate	Intense	Medium	Moderate
%	10	21	68	10	24	66
Erg	43	20	6	38	0	1
Calcareous	57	73	62	62	63	20
Chott	0	6	33	0	38	79

to better understand their past, present, and future role on marine biochemistry, and, beyond, on the Earth's climate.

Declarations

Conflict of interest The authors declare no competing interests.

References

Abed AM, Al Kuisi M, Khair HA (2009) Characterization of the Khamaseen (spring) dust in Jordan. Atmos Environ 43:2868–2876. https://doi.org/10.1016/j.atmosenv.2009.03.015

AL-Harbi M (2015) Characteristics and composition of the falling dust in urban environment. Int J Environ Sci Technol. https://doi.org/10.1007/s13762-013-0440-8

Alfaro SC, Abdel Wahab M (2005) Extreme variability of aerosol optical properties: The cairo aerosol characterization experiment case study. In: NATO security through science series C: environmental security

Alfaro SC, Gaudichet A, Rajot JL et al (2003a) Variability of aerosol size-resolved composition at an Indian coastal site during the Indian Ocean Experiment (INDOEX) intensive field phase. J Geophys Res Atmos. https://doi.org/10.1029/2002jd002645

Alfaro SC, Gomes L, Rajot JL et al (2003b) Chemical and optical characterization of aerosols measured in spring 2002 at the ACE-Asia supersite, Zhenbeitai, China. J Geophys Res Atmos. https://doi.org/10.1029/2002JD003214

Ammar K, El-Metwally M, Almazroui M, Abdel Wahab MM (2014) A climatological analysis of Saharan cyclones. Clim Dyn 43:483–501. https://doi.org/10.1007/s00382-013-2025-0

Balkanski Y, Schulz M, Claquin T, Guibert S (2007) Reevaluation of Mineral aerosol radiative forcings suggests a better agreement with satellite and AERONET data. Atmos Chem Phys 7:81–95. https://doi.org/10.5194/acp-7-81-2007,2007

Basart S, PéRez C, Nickovic S et al (2012) Development and evaluation of the BSC-DREAM8b dust regional model over northern Africa, the mediterranean and the middle east. Tellus Ser B Chem Phys Meteorol. https://doi.org/10.3402/tellusb.v64i0.18539

Ben-Israel M, Enzel Y, Amit R, Erel Y (2015) Provenance of the various grain-size fractions in the Negev loess and potential changes in major dust sources to the Eastern Mediterranean. Quat Res 83:105–115. https://doi.org/10.1016/j.yqres.2014.08.001

Bian H, Zender CS (2003) Mineral dust and global tropospheric chemistry: relative roles of photolysis and heterogeneous uptake. J Geophys Res Atmos. https://doi.org/10.1029/2002JD003143

Bibi M, Saad M, Masmoudi M et al (2020) Long-term (1980–2018) spatial and temporal variability of the atmospheric dust load and deposition fluxes along the North-African coast of the Mediterranean Sea. Atmos Res 234:104689

Bowen HJM (1966) Trace elements in biochemistry. Academic Press, London, p 241

Caquineau S, Gaudichet A, Gomes L, Legrand M (2002) Mineralogy of Saharan dust transported over northwestern tropical Atlantic Ocean in relation to source regions. J Geophys Res Atmos 107:AAC 4-1-AAC 4-12. https://doi.org/10.1029/2000JD000247

Cassar N, Bender ML, Barnett BA et al (2007) The southern ocean biological response to aeolian iron deposition. Science (80-) 317:5. https://doi.org/10.1126/science.1144602

Dentener FJ, Carmichael GR, Zhang Y et al (1996) Role of mineral aerosol as a reactive surface in the global troposphere. J Geophys Res Atmos 101:22869–22889

Ehrmann W, Schmiedl G (2021) Nature and dynamics of North African humid and dry periods during the last 200,000 years documented in the clay fraction of Eastern Mediterranean deep-sea sediments. Quat Sci Rev 260:106925. https://doi.org/10.1016/j.quascirev.2021.106925

El-Metwally M, Alfaro SC (2013) Correlation between meteorological conditions and aerosol characteristics at an East-Mediterranean coastal site. Atmos Res 132:76–90. https://doi.org/10.1016/j.atmosres.2013.05.006

El-Metwally M, Alfaro SC, Wahab MMA et al (2010) Seasonal and inter-annual variability of the aerosol content in Cairo (Egypt) as deduced from the comparison of MODIS aerosol retrievals with direct AERONET measurements. Atmos Res 97:14–25. https://doi.org/10.1016/j.atmosres.2010.03.003

El-Metwally M, Alfaro SC, Wahab MMA et al (2011) Aerosol properties and associated radiative effects over Cairo (Egypt). Atmos Res 99:263–276. https://doi.org/10.1016/j.atmosres.2010.10.017

El-Metwally M, Korany M, Boraiy M et al (2020) Evidence of anthropization of aerosols in the Saharan and peri-Saharan regions: implications for the atmospheric transfer of solar radiation. J Atmos Solar Terrestrial Phys 199:105199. https://doi.org/10.1016/j.jastp.2020.105199

El-Wakil SA, El-Metwally M, Gueymard C (2001) Atmospheric turbidity of urban and desert areas of the Nile Basin in the aftermath of Mt. Pinatubo's eruption. Theor Appl Climatol 68:89–108. https://doi.org/10.1007/s007040170056

El-Askary H, Kafatos M (2008) Dust storm and black cloud influence on aerosol optical properties over Cairo and the Greater Delta region, Egypt. Int J Remote Sens 29:7199–7211. https://doi.org/10.1080/01431160802144179

El-Metwally M, Alfaro SC, Abdel Wahab M, Chatenet B (2008) Aerosol characteristics over urban Cairo: seasonal variations as retrieved from Sun photometer measurements. J Geophys Res Atmos. https://doi.org/10.1029/2008JD009834

Favez O, Cachier H, Sciare J et al (2008) Seasonality of major aerosol species and their transformations in Cairo megacity. Atmos Environ 42:1503–1516. https://doi.org/10.1016/j.atmosenv.2007.10.081

Formenti P, Rajot JL, Desboeufs K et al (2008) Regional variability of the composition of mineral dust from western Africa: Results from the AMMA SOP0/DABEX and DODO field campaigns. J Geophys Res Atmos. https://doi.org/10.1029/2008JD009903

Ganor E, Foner HA (1996) The mineralogical and chemical properties and the behaviour of aeolian Saharan dust over Israel. In: Guerzoni S, Chester R (eds) The Impact of Desert Dust Across the Mediterranean. Environmental Science and Technology Library, vol. 11 Springer, Dordrecht. https://doi.org/10.1007/978-94-017-3354-0_15

Global Modelling and Assimilation Offfice (2018) MERRA-2 reanalysis. In: Web site 10.5067/FH9A0MLJPC7N. Accessed 18 July 2022

Griffin DW, Garrison VH, Herman JR, Shinn EA (2001) African desert dust in the Caribbean atmosphere: microbiology and public health. Aerobiologia (bologna) 17:203–213. https://doi.org/10.1023/A:1011868218901

Hamimi Z, El-Barkooky A, Frías JM et al (2020) The geology of Egypt. Springer, London

Henderson P, Henderson G (2009) Cambridge handbook of earth science data. Cambridge University Press, Cambridge

Hudson-Edwards KA, Bristow CS, Cibin G et al (2014) Solid-phase phosphorus speciation in Saharan Bodélé Depression dusts and source sediments. Chem Geol. https://doi.org/10.1016/j.chemgeo.2014.06.014

Issanova G, Abuduwaili J, Galayeva O et al (2015) Aeolian transportation of sand and dust in the Aral Sea region. Int J Environ Sci Technol. https://doi.org/10.1007/s13762-015-0753-x

Jickells TD, An ZS, Andersen KK et al (2005) Global iron connections between desert dust, ocean biogeochemistry, and climate. Science (80-) 308:67–71. https://doi.org/10.1126/science.1105959

Journet E, Balkanski Y, Harrison SP (2014) A new data set of soil mineralogy for dust-cycle modeling. Atmos Chem Phys 14:3801–3816. https://doi.org/10.5194/acp-14-3801-2014

Kandler K, Schütz L, Deutscher C et al (2009) Size distribution, mass concentration, chemical and mineralogical composition and derived optical parameters of the boundary layer aerosol at Tinfou, Morocco, during SAMUM 2006. Tellus B Chem Phys Meteorol 61:32–50. https://doi.org/10.1111/j.1600-0889.2008.00385.x

Knippertz P, Evans MJ, Field PR et al (2015) The possible role of local air pollution in climate change in West Africa. Nat Clim Change. https://doi.org/10.1038/nclimate2727

Knippertz P, Stuut J-BW (2014) Mineral dust: a key player in the earth system. Springer, New York

Kumar P, Sokolik IN, Nenes A (2011) Measurements of cloud condensation nuclei activity and droplet activation kinetics of fresh unprocessed regional dust samples and minerals. Atmos Chem Phys 11:3527–3541. https://doi.org/10.5194/acp-11-3527-2011

Lafon S, Alfaro SC, Chevaillier S, Rajot JL (2014) A new generator for mineral dust aerosol production from soil samples in the laboratory: GAMEL. Aeolian Res 15:319–334

Laurent B, Marticorena B, Bergametti G et al (2008) Modeling mineral dust emissions from the Sahara desert using new surface properties and soil database. J Geophys Res Atmos. https://doi.org/10.1029/2007JD009484

Li J, Okin GS, Alvarez L, Epstein H (2007) Quantitative effects of vegetation cover on wind erosion and soil nutrient loss in a desert grassland of southern New Mexico, USA. Biogeochemistry. https://doi.org/10.1007/s10533-007-9142-y

Linke C, Möhler O, Veres A et al (2006) Optical properties and mineralogical composition of different Saharan mineral dust samples: a laboratory study. Atmos Chem Phys 6:3315–3323. https://doi.org/10.5194/acp-6-3315-2006

Maenhaut W, Salma I, Cafmeyer J et al (1996) Regional atmospheric aerosol composition and sources in the eastern Transvaal, South Africa, and impact of biomass burning. J Geophys Res Atmos. https://doi.org/10.1029/95jd02930

Mailler S, Menut L, Khvorostyanov D et al (2017) CHIMERE-2017: from urban to hemispheric chemistry-transport modeling. Geosci Model Dev 10:2397–2423. https://doi.org/10.5194/gmd-10-2397-2017

Marconi M, Sferlazzo DM, Becagli S et al (2014) Saharan dust aerosol over the central Mediterranean Sea: PM 10 chemical composition and concentration versus optical columnar measurements. Atmos Chem Phys 14:2039–2054. https://doi.org/10.5194/acp-14-2039-2014

Masmoudi M, Alfaro SC, El Metwally M (2015) A comparison of the physical properties of desert dust retrieved from the sunphotometer observation of major events in the Sahara, Sahel, and Arabian Peninsula. Atmos Res. https://doi.org/10.1016/j.atmosres.2015.02.005

Menut L, Siour G, Bessagnet B et al (2020) Modelling the mineralogical composition and solubility of mineral dust in the Mediterranean area with CHIMERE 2017r4. Geosci Model Dev 13:2051–2071. https://doi.org/10.5194/gmd-13-2051-2020

Morman SA, Plumlee GS (2013) The role of airborne mineral dusts in human disease. Aeolian Res 9:203–212

Mostafa AN, Zakey AS, Alfaro SC et al (2019) Validation of RegCM-CHEM4 model by comparison with surface measurements in the Greater Cairo (Egypt) megacity. Environ Sci Pollut Res 26:23524–23541. https://doi.org/10.1007/s11356-019-05370-0

Moulin C, Lambert CE, Dayan U et al (1998) Satellite climatology of African dust transport in the Mediterranean atmosphere. J Geophys Res Atmos 103:13137–13144. https://doi.org/10.1029/98JD00171

Okin GS, Mahowald N, Chadwick OA, Artaxo P (2004) Impact of desert dust on the biogeochemistry of phosphorus in terrestrial ecosystems. Global Biogeochem Cycles. https://doi.org/10.1029/2003GB002145

Pastore G, Baird T, Vermeesch P et al (2021) Provenance and recycling of Sahara Desert sand. Earth Sci Rev 216:103606

Rajot JL, Formenti P, Alfaro S et al (2008) AMMA dust experiment: An overview of measurements performed during the dry season special observation period (SOP0) at the Banizoumbou (Niger)

supersite. J Geophys Res Atmos. https://doi.org/10.1029/2008J D009906

Richon C, Dutay J-C, Dulac F et al (2018) Modeling the impacts of atmospheric deposition of nitrogen and desert dust-derived phosphorus on nutrients and biological budgets of the Mediterranean Sea. Prog Oceanogr 163:21–39. https://doi.org/10.1016/j.pocean.2017.04.009

Rodríguez S, Alastuey A, Alonso-Pérez S et al (2011) Transport of desert dust mixed with North African industrial pollutants in the subtropical Saharan Air Layer. Atmos Chem Phys 11:6663–6685. https://doi.org/10.5194/acp-11-6663-2011

Saad M, Masmoudi M, Chevaillier S et al (2018) Variability of the elemental composition of airborne mineral dust along the coast of Central Tunisia. Atmos Res 209:170–178

Schepanski K (2018) Transport of Mineral Dust and Its Impact on Climate. Geosciences 8:151. https://doi.org/10.3390/geoscience s8050151

Scheuvens D, Schütz L, Kandler K et al (2013) Bulk composition of northern African dust and its source sediments—a compilation. Earth Sci Rev 116:170–194

Schulz M, Prospero JM, Baker AR et al (2012) Atmospheric transport and deposition of mineral dust to the ocean: Implications for research needs. Environ Sci Technol 46:10390–10404. https://doi.org/10.1021/es300073u

Sokolik IN, Winker DM, Bergametti G et al (2001) Introduction to special section: Outstanding problems in quantifying the radiative impacts of mineral dust. J Geophys Res Atmos 106:18015–18027. https://doi.org/10.1029/2000JD900498

Stein AF, Draxler RR, Rolph GD et al (2015) NOAA's HYSPLIT atmospheric transport and dispersion modeling system. Bull Am Meteorol Soc 96:2059–2077. https://doi.org/10.1175/BAMS-D-14-00110.1

Suresh K, Kumar A, Ramaswamy V et al (2022) Seasonal variability in aeolian dust deposition fluxes and their mineralogical composition over the Northeastern Arabian Sea. Int J Environ Sci Technol 19:7701–7714. https://doi.org/10.1007/s13762-021-03503-y

Swap R, Garstang M, Greco S et al (1992) Saharan dust in the Amazon Basin. Tellus B 44:133–149. https://doi.org/10.3402/tellusb.v44i2.15434

Taylor SR (1964) Abundance of chemical elements in the continental crust: a new table. Geochim Cosmochim Acta 28:1273–1285

Varkitzi I, Psarra S, Assimakopoulou G et al (2020) Phytoplankton dynamics and bloom formation in the oligotrophic Eastern Mediterranean: field studies in the Aegean, Levantine and Ionian seas. Deep Sea Res Part II Top Stud Oceanogr 171:104662

Wheida A, Nasser A, El Nazer M et al (2018) Tackling the mortality from long-term exposure to outdoor air pollution in megacities: Lessons from the Greater Cairo case study. Environ Res 160:223–231

Zhao A, Ryder CL, Wilcox LJ (2022) How well do the CMIP6 models simulate dust aerosols? Atmos Chem Phys 22:2095–2119. https://doi.org/10.5194/acp-22-2095-2022